Research Article | Vol. 27, No. 17 | 19 Aug 2019 | OPTICS EXPRESS 23654
Optics EXPRESS

Compact polarization diversity Kramers-Kronig coherent receiver on silicon chip

FAN ZHANG,[1,3] XIAOKE RUAN,[1] YIXIAO ZHU,[1] ZEYU CHEN,[1] XIAOMING QIU,[1] FAN YANG,[1] KE LI,[2] AND YANPING LI[1,4]

[1]*State Key Laboratory of Advanced Optical Communication Systems and Networks, Department of Electronics, Nano-optoelectronics Frontier Center of the Ministry of Education, Peking University, Beijing 100871, China*
[2]*Optoelectronics Research Centre, University of Southampton, Southampton SO17 1BJ, UK*
[3]*fzhang@pku.edu.cn*
[4]*liyp@pku.edu.cn*

Abstract: We design and fabricate a compact silicon photonic integrated circuit (PIC) for polarization diversity heterodyne coherent detection. This PIC integrates two optical gratings for fiber coupling and polarization diversity, two germanium single-ended photodetectors (PDs), and three multimode interferometers (MMIs) for power splitting and optical hybrid. The device is highly compact with a footprint of 0.68mm × 0.9mm. We test this PIC with heterodyne detection experiments of polarization division multiplexed (PDM) 32Gbaud quadrature phase shift keying (QPSK) and 16-ary quadrature amplitude modulation (16QAM) signals. The signal-signal beat interference due to square-law detection is separately mitigated with the Kramers-Kronig (KK) scheme for each of the two orthogonal polarizations. To our best knowledge, we report the first PDM-KK coherent receiver in PIC with a capability of detecting 256Gb/s 16QAM signals, which shows the most compact size among the silicon coherent receivers ever reported.

1. Introduction

Coherent receiver can either use intradyne or heterodyne detection. Intradyne detection for polarization division multiplexed (PDM) quadrature amplitude modulation (QAM) signals usually requires two 90-degree optical hybrids and four balanced photodetector (PD) pairs to accommodate both polarization and phase diversity for in-phase/quadrature (I/Q) components of two orthogonal polarizations. In contrast, heterodyne detection retrieves the up-converted I/Q components simultaneously in the intermediate frequency (IF). Compared with intradyne detection, heterodyne detection reduces half of the balanced PD pairs at the cost of the PD bandwidth at least doubled. To further simplify the receiver structure, the single-ended instead of the balanced PD pairs can be implemented, which, however, suffers signal-signal beat interference (SSBI) caused by square-law detection [1]. Thanks to the Kramers-Kronig (KK) receiver [1], the signal phase can be retrieved from the amplitude waveform, given a single sideband (SSB) and minimum phase signal. In doing so, the polarization diversity heterodyne coherent receiver can be simplified with only two single-ended PDs [2]. So far, the previously reported PDM-KK receivers are implemented with commercial discrete components [2,3].

In the last decade, the silicon photonic integrated circuit (PIC) attracts extensive studies for coherent receivers due to its compactness, low cost and low power consumption, which is of great importance for pluggable modules in high density data center interconnect. The first silicon PIC of intradyne coherent receiver was reported in 2010 [4], which was tested with PDM quadrature phase shift keying (QPSK) signals operating at 43Gb/s and 112Gb/s. The PIC includes four 2 × 2 multimode interference (MMI) couplers for 90-degree optical hybrid. The outputs of the MMI couplers proceed to four germanium (Ge) PD pairs. The chip size is

#364239 https://doi.org/10.1364/OE.27.023654
Journal © 2019 Received 8 Apr 2019; revised 30 Jun 2019; accepted 24 Jul 2019; published 5 Aug 2019

Optics EXPRESS

1.6mm × 3.6mm [4]. In 2013, a silicon PIC coherent receiver was demonstrated with a capability of detecting 224-Gb/s PDM 16QAM signals, which includes two 4 × 4 MMIs for 90-degree optical hybrid and has a chip size of 1.3mm × 3.0mm [5]. Recently, some studies are reported to reduce the footprint of coherent receivers. In 2017, a 90-degree optical hybrid comprising one Y-junction and three 2x2 MMI couplers on silicon was presented with a compact footprint of 21.6μm × 27.9μm [6]. In 2018, silicon photonic 90-degree inter-polarization mixers with a small footprint of 145μm × 60μm was demonstrated [7].

In this work, we report the first silicon PIC for polarization diversity Kramers-Kronig heterodyne detection. One 1 × 2 MMI is used for power splitting and two 2 × 2 MMIs are applied for optical hybrids. Two single-ended Ge PDs are employed for detecting X and Y polarizations, respectively. We test the PIC chip with 32Gbaud PDM QPSK/16QAM signals. With a size of 0.68 mm × 0.9mm, its footprint is about one sixth of that of typical silicon PIC intradyne receivers [4,5]. This PIC is the most compact silicon receiver capable of detecting 256Gb/s PDM 16QAM signals.

2. Device layout and characteristics

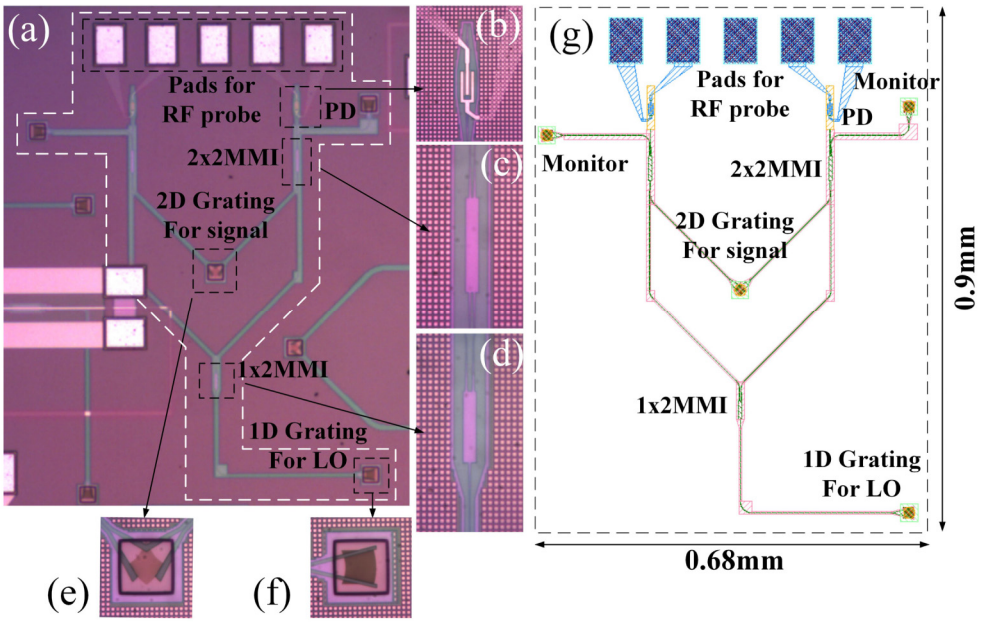

Fig. 1. (a) Photograph of the PIC (highlighted by the white dashed line). The zoom-in photographs of (b) the single-ended PD; (c) 2 × 2 MMI; (d) 1 × 2 MMI; (e) the 2D grating coupler; (f) the 1D grating coupler. (g) The layout of the PIC.

Figure 1 shows the photograph and the layout of the silicon PIC fabricated with IMEC's ISIPP50G technology. In Fig. 1(a), the PIC is highlighted by the white dashed line. The waveguides are 220-nm-high crystalline silicon strips with 1.0μm-thick oxide upper cladding and 2.0μm-thick oxide lower cladding on a 725μm-height silicon substrate. The chip is tested without electrical or optical packaging. The signal and the local oscillator (LO) laser enter the chip vertically through the optical grating couplers, respectively. For the LO, a one-dimensional (1-D) optical grating with an insertion loss about 5.0 dB is used for fiber coupling and a 1 × 2 MMI with an extra loss about 1.0 dB is used for power splitting. The PDM signals are coupled to the chip in TE mode through a two-dimensional (2D) optical grating that has a constant coupling efficiency for light of any polarization [4]. The measured insertion loss of our 2D grating is about 7dB. Two 2 × 2 MMIs with extra loss about 1.0 dB are used for optical hybrids of the LO and the signals in both X and Y polarizations. Two

Optics EXPRESS

single-ended Ge PDs are used for detecting the signals in X and Y polarizations, respectively. A group of GSGSG pads are built for detecting high-speed electrical signals through the radio frequency (RF) probe. Figures 1(b)–1(f) show zoom-in photographs of the single-ended PD, 2 × 2 MMI, 1 × 2 MMI, 2D grating coupler, and 1D grating coupler, respectively. The layout of the PIC is also illustrated in Fig. 1(g). One of the outputs of 2 × 2 MMI is connected with a 1D grating coupler as a monitor for optical power. Taking the two monitors into account, the footprint of the whole structure is about 0.68 mm × 0.9mm. For practical device, the monitors can be removed. Moreover, the positions of 1D and 2D couplers are designed for fiber holders in our experiment. With optical packaging, the positions of 1D and 2D couplers can be optimized to further reduce the PIC size.

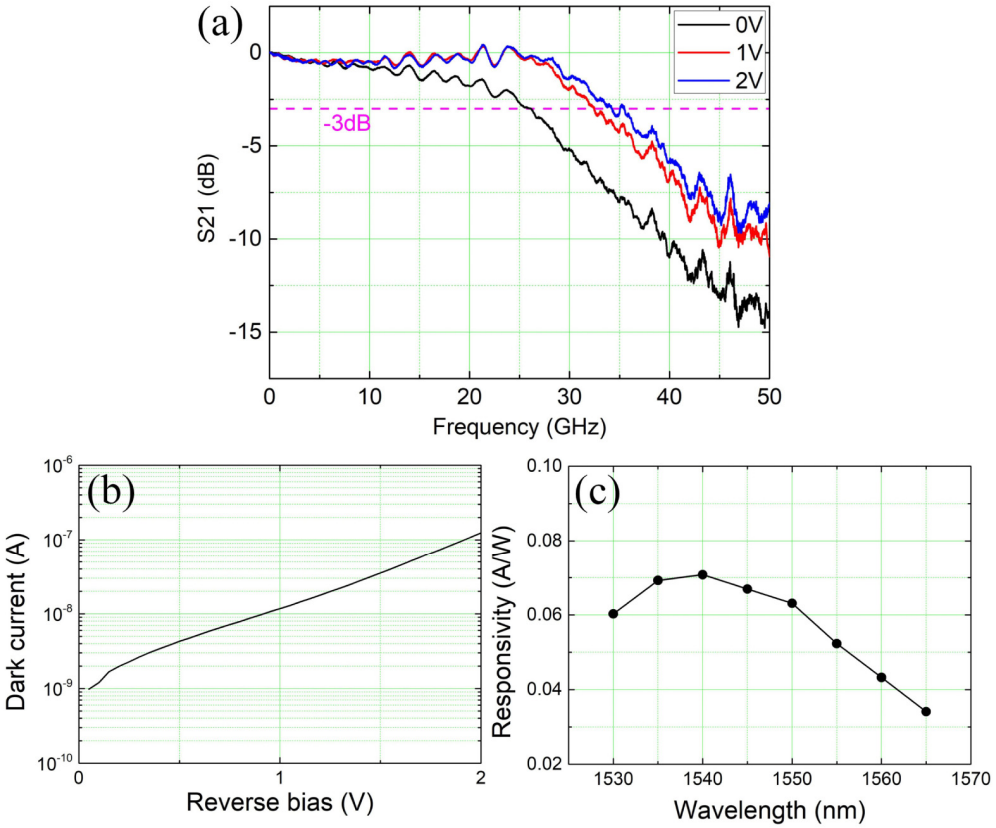

Fig. 2. The characteristic of the PIC. (a) Electro-optic response of the photodetector at various reverse bias voltages. (b) Dark current as a function of the reverse bias. (c) Measured fiber-to-PD responsivity.

Figure 2 shows the characteristic of the PIC. Figure 2(a) shows the bandwidths of the Ge PD under different bias voltages, which are measured by using a network analyzer (Keysight N5247A) and a commercial modulator after calibration. With the reverse bias voltage varying from 0 to 2.0V, the 3-dB bandwidth of the photodetector gradually increases from 25.8 GHz to 34.3 GHz. The increased bandwidth is mainly due to the reduction of lateral p-n junction capacitance, which is analogous to the reduction of resistor-capacitor (RC) time constant. In the following experiments, we choose 2.0V as the reverse bias.

The dark current of the Ge PD is collected and presented in Fig. 2(b). The dark current is ~100nA at the reverse bias of 2.0V, which has little influence on the received signal. We also measure the fiber-to-PD responsivities at different wavelength under 2.0V reverse bias, which is shown in Fig. 2(c). The peak responsivity is ~0.071 A/W at 1540 nm, which is not only

Optics EXPRESS

decided by the wavelength sensitivity of the germanium's optical absorption coefficient, but also influenced by the wavelength sensitivity of the grating couplers.

3. Heterodyne system experiments

3.1. Experimental setup

Figure 3 shows the experiment setup to test the PIC receiver. At the transmitter, an external cavity laser (ECL) with ~100 kHz linewidth is used as the optical source. The arbitrary waveform generator (AWG) (Keysight M8195A) operating at 64GSa/s generates 32GBaud baseband Nyquist 16QAM (or QPSK) signal. The IQ modulator is biased at the null point. A polarization-maintaining erbium-doped optical fiber amplifier (PM-EDFA) is used to amplify the modulated signal. PDM is emulated with a polarization beam splitter/combiner (PBS/PBC) and a tunable optical delay line. The delay of the optical delay line is measured as 130 symbols. At the receiver, an optical band-pass filter (OBPF) (Yenista XTM-50) is used to remove out-of-band amplifier spontaneous emission (ASE) noise. The outputs of the silicon PDM-KK receiver are amplified by two electrical amplifiers (EAs) (SHF-S807) with ~50GHz bandwidth. A digital storage oscilloscope (DSO) (Keysight DSA-X 96204Q) operating at 160GSa/s is employed to capture the waveforms for off-line digital signal processing (DSP).

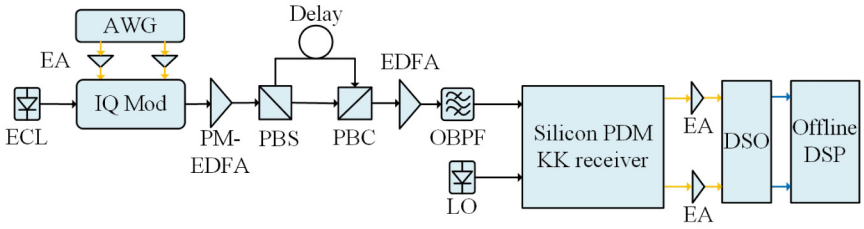

Fig. 3. Experimental setup to test the silicon PDM KK receiver.

3.2. DSP stack

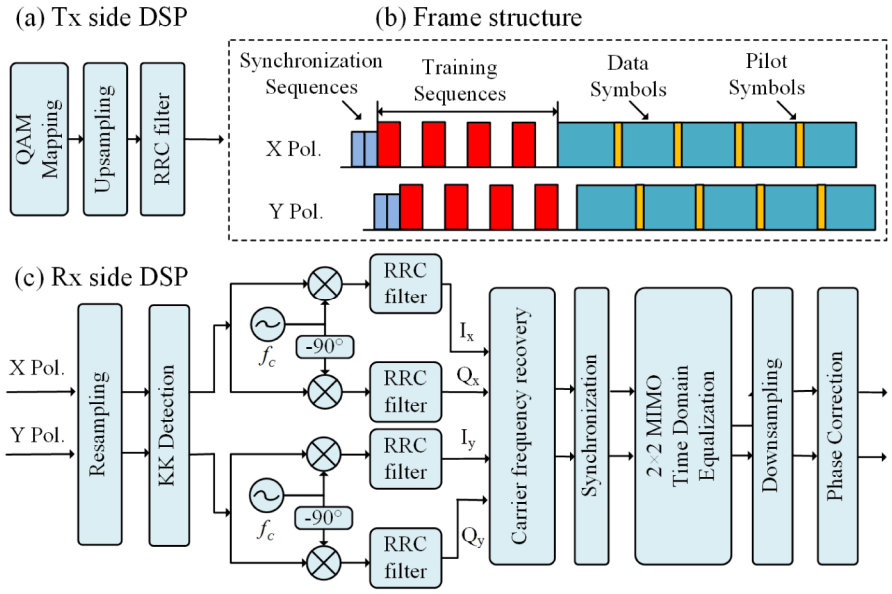

Fig. 4. (a) Transmitter-side DSP; (b) Frame structure; (c) Receiver-side DSP.

Figures 4(a)–4(c) show the transmitter and the receiver DSP and the data frame structure. At the transmitter, the bit stream is mapped to 16QAM (or QPSK) first. After 2 times up-

Optics EXPRESS

sampling, the signal is digitally shaped using root raise cosine (RRC) filter with a roll-off factor of 0.01. The preamble includes two 64-symbol synchronization sequences and four 130-symbol training sequences. 35840 data symbols are transmitted after the preamble. For coarse phase estimation, we uniformly insert two pilots for each block of 128 data symbols. Therefore, the net bit rate of a single carrier is 228.1 (32 × 4 × 2/1.07/(64 × 2 + 130 × 2 × 4 + 128 × 280) × 126 × 280)Gb/s with consideration of both frame redundancy and the 7% hard-decision forward error correction (HD-FEC) threshold.

At the receiver, the signal is firstly re-sampled to 4 samples per symbol (SPS). The SSBI of each polarization is separately overcome with the KK scheme. After SSBI compensation, the signal is down-converted by the frequency f_C and filtered by a matched RRC filter. f_C is the frequency offset between the signal and the LO. The residual frequency offset is estimated by calculating the maximum of $\left|\mathrm{FFT}\left(r^4(t)\right)\right|$. $\mathrm{FFT}(\cdot)$ is the fast Fourier transformation and $r(t)$ is the down-converted signal. After synchronization, the signals of two polarizations are equalized with a Ts/2 (Ts is the symbol period) spaced 2 × 2 multi-input-multi-output (MIMO) training sequence-based time domain equalization. The carrier phase recovery is performed first with coarse phase tracking using the uniformly distributed pilots and then accurate recovery based on the blind phase search algorithm [2]. Finally, the bit error rate (BER) is calculated by error counting based on a total of ~1.4×10^6 bits.

3.3. Results

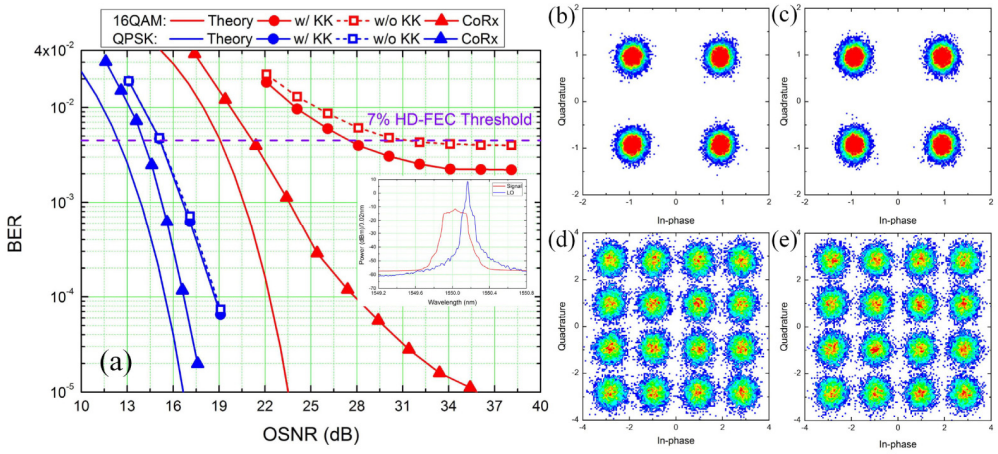

Fig. 5. (a) The measured BER as a function of the OSNR for both 32Gbaud QPSK (128Gb/s) and 32Gbaud 16QAM (256Gb/s) signals. Typical constellations with KK detection of (b) X-polarization QPSK; (c) Y-polarization QPSK; (d) X-polarization 16QAM; (e) Y-polarization 16QAM. The OSNR values are both 38.1dB for Figs. 5(b)–5(e).

Figure 5(a) shows the measured BER as a function of optical signal to noise ratio (OSNR) for 32Gbaud QPSK/16QAM signals with and without KK operation at back-to-back (BTB) scenarios, respectively. An intradyne coherent receiver (CoRx) consisting of discrete photodiodes (FINISAR BPDV3120R) and optical hybrid is tested for comparison. The discrete photodiodes have a bandwidth about 70GHz and subsequently amplified by the same electrical amplifiers (SHF S807) with that used in our PIC test. The theoretical curves for both QPSK and 16QAM are also shown. The insert is the optical spectra at the receiver with 0.02nm resolution. The signal and the LO operate at 1550.03nm and 1550.16nm, respectively. $f_C \approx 0.51 f_S$, where f_S is the symbol rate. The LO wavelength is set close to the signal edge to construct a nearly half-cycle SSB signal before PD detection. The LO-to-signal power ratio (LOSPR) is set as ~12 dB to ensure the minimum phase condition for KK detection [1]. For

Optics EXPRESS

QPSK signal (the blue curves), the OSNR penalty with KK detection is about 2.7dB compared with the theoretical curve at a BER target of 4.5×10^{-3} for the 7% HD-FEC threshold [8]. Note that there is little improvement for QPSK signal with KK detection. The reason is that the BER is limited by ASE noise rather than SSBI when the OSNR is below 20.0dB. For 16QAM signal (the red curves), a 3.8dB OSNR penalty improvement can be observed after applying KK operation. The implementation penalty of the PDM-KK receiver for 16QAM signal is about 8.5dB compared with the theoretical curve at a BER of 4.5×10^{-3}. Compared with the discrete CoRx, the PIC shows worse performance and there is an error floor for 16QAM test when the OSNR is larger than 34.0dB, which is mainly caused by the noise of the integrated Ge PDs.

Figures 5(b)–5(e) show the typical constellations of X and Y polarizations of 32Gbaud PDM QPSK/16QAM signals with KK receiver, respectively. Both of the two polarizations demonstrate similar performance. 32Gbaud QPSK clearly shows an error-free operation. In contrast, 32Gbaud 16QAM signals in both X and Y polarizations demonstrate divergent constellations that correspond to the BER floor in Fig. 5(a).

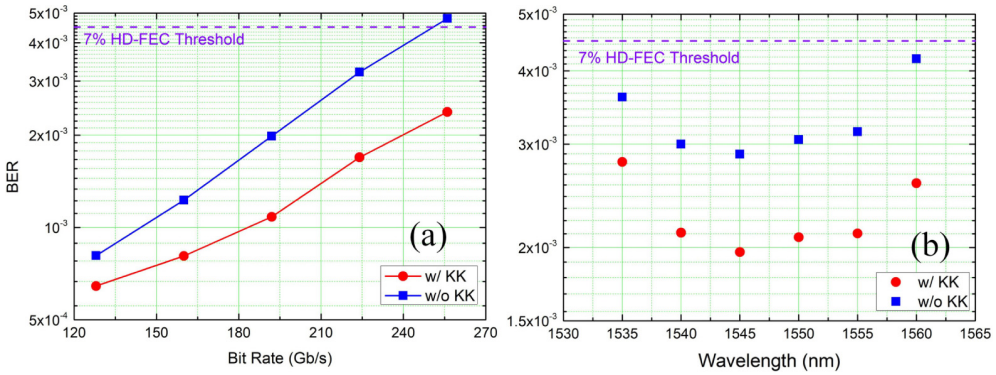

Fig. 6. Measured BERs of 16QAM signals for (a) different bit rates at 1550nm; (b) six wavelengths from 1535nm to 1560nm for 32Gbaud 16QAM signals.

Figure 6(a) shows the measured BERs versus different bit rates for 16QAM signal with and without KK detection, respectively, at BTB scenarios. The OSNR is measured as 41.0dB. After applying the KK detection for SSBI mitigation, the BERs are 6.4×10^{-4}, 8.1×10^{-4}, 1.1×10^{-3}, 1.7×10^{-3} and 2.4×10^{-3} for bit rates of 128Gb/s, 160Gb/s, 192Gb/s, 224Gb/s and 256Gb/s, respectively. With 7% HD-FEC, this PIC can support the error-free detection of 16QAM signals as high as 256Gb/s.

Figure 6(b) displays the BERs with different wavelengths for 32Gbaud 16QAM signal at BTB scenario. The OSNR is measured as 41.0dB. All the BERs are below the 7% HD-FEC threshold when operating at C band. To be specific, the silicon PDM-KK receiver has its best performance at the wavelength range of [1540nm 1555nm], where the BER is ~2.1×10^{-3} by using KK detection. For the wavelength operating around 1535nm and 1560nm, the BER performance becomes worse due to the coupling loss increase of the optical gratings.

Note that a heterodyne receiver can also be implemented with quasi-balanced PDs to remove SSBI and other common mode noise by subtraction, which, however, demands high common mode rejection ratio (CMRR) between two branches. The CMRR can be further adjusted by differential transimpedance amplifier (TIA) with automatic gain control to cancel the imbalance between two separate PDs [9]. Although quasi-balanced PDs and differential TIAs with high CMRR can achieve better performance, two separate direct current (DC) pads on both optical and electrical chips must be designed for TIAs being coupled to the DC bias of two cathodes of quasi-balanced PDs, which brings the concerns with packaging complexity and reliability. Moreover, the pad area on any electrical complementary metal Oxide

Optics EXPRESS

semiconductor (CMOS) chip cannot be ignored. Instead of subtracting SSBI with quasi-balanced PD or differential TIA, we eliminate SSBI by the KK detection. Therefore, we do not need to consider the CMRR issue, which simplify our PIC design significantly.

4. Conclusions

In conclusion, we report the first silicon PIC for polarization diversity heterodyne coherent detection. With the KK scheme, this PIC device is capable of detecting 256 Gb/s PDM 16QAM signals with two single-ended PDs. Compared with conventional silicon PIC intradyne receiver with four balanced PDs, this PIC heterodyne receiver simplifies the optical frontend by using two single-ended PDs with doubled bandwidth. To our best knowledge, it is the most compact PDM coherent receiver in PIC, which is of great importance for high density optical interconnect.

Funding

National Natural Science Foundation of China (61535002).

References

1. A. Mecozzi, C. Antonelli, and M. Shtaif, "Kramers-Kronig coherent receiver," Optica **3**(11), 1220–1227 (2016).
2. Y. Zhu, K. Zou, X. Ruan, and F. Zhang, "'Single Carrier 400G Transmission with Single-ended Heterodyne Detection," IEEE Photonics Technol. Lett. **29**(21), 1788–1791 (2017).
3. X. Chen, C. Antonelli, S. Chandrasekhar, G. Raybon, A. Mecozzi, M. Shtaif, and P. Winzer, "Kramers–Kronig Receivers for 100-km Datacenter Interconnects," J. Lightwave Technol. **36**(1), 79–89 (2018).
4. C. R. Doerr, P. Winzer, Y. Chen, S. Chandrasekhar, M. S. Rasras, L. Chen, T. Liow, K. Ang, and G. Lo, "Monolithic Polarization and Phase Diversity Coherent Receiver in Silicon," J. Lightwave Technol. **28**(4), 520–525 (2010).
5. P. Dong, X. Liu, S. Chandrasekhar, L. L. Buhl, R. Aroca, Y. Baeyens, and Y. Chen, "224-Gb/s PDM-16-QAM modulator and receiver based on silicon photonic integrated circuits," in *Optical Fiber Communication Conference and Exposition and the National Fiber Optic Engineers Conference (OFC/NFOEC)* (Optical Society of America, 2013), pp. 1–3.
6. H. Guan, Y. Ma, R. Shi, X. Zhu, R. Younce, Y. Chen, J. Roman, N. Ophir, Y. Liu, R. Ding, T. Baehr-Jones, K. Bergman, and M. Hochberg, "Compact and low loss 90°optical hybrid on a silicon-on-insulator platform," Opt. Express **25**(23), 28957–28968 (2017).
7. A. Melikyan, K. Kim, N. Fontaine, S. Chandrasekhar, Y. K. Chen, and P. Dong, "Inter-polarization mixers for coherent detection of optical signals," Opt. Express **26**(14), 18523–18531 (2018).
8. F. Chang, K. Onohara, and T. Mizuochi, "Forward error correction for 100 G transport networks," IEEE Commun. Mag. **48**(3), S48–S55 (2010).
9. A. Awny, R. Nagulapalli, M. Kroh, J. Hoffmann, P. Runge, D. Micusik, G. Fischer, A. C. Ulusoy, M. Ko, and D. Kissinger, "A linear differential transimpedance amplifier for 100-Gb/s integrated coherent optical fiber receivers," IEEE Trans. Microw. Theory Tech. **66**(2), 973–986 (2018).